COMPARATIVE STUDY OF $LA_{0.7}CA_{0.3}MN_{0.95}FE_{0.05}O_3$ PEROVSKITES PREPARED BY DIFFERENT METHODS AND EFFECT OF PREPARATION ON CATALYTIC ACTIVITY FOR HYDROXYLATION OF BENZENE

MOHAMED S. THABET

.*Department of Chemistry, Faculty of Science, Al-Azhar University, Cairo, Egypt*

E-mail address: thabet1972@yahoo.com

Abstract

Magnetic nanoparticles of $La_{0.7}Ca_{0.3}Mn_{0.95}Fe_{0.05}O_3$ perovskites were synthesized by various wet chemical routes, namely co-precipitation, oxalate-gel and citrate-gel methods. Phase formation and crystal structure of the synthesized powders were examined by the X-ray diffraction (XRD) using the Rietveld analysis. The micro- structure was determined by means of scanning electron microscopy (SEM). Infrared transmission spectroscopy revealed that stretching and bending modes are influenced by preparation methods. Synthesis using the oxalate-gel method yielded incomplete reaction irrespective of the calcination temperature adopted. The citrate-gel method yielded better powder properties in terms of particle size and morphology as compared to co-precipitation synthesis. The highest activity for the catalytic oxidation of benzene to phenol in presence of H_2O_2 was obtained with the sample prepared by the citrate–gel method.

Keywords: XRD, perovskites, catalytic activity, hydroxylation of benzene, SEM

Introduction

A large research effort has been devoted in recent years to manganese oxides to take advantage of their interesting properties, i.e. metal to insulator transition and colossal magnetoresistance (CMR). Doped manganites, with the general formula $Ln_{1-x}Ca_xMnO_3$ (Ln = Sr, La) have been intensively studied, as they are considered as potential candidates for industrial applications [1]. Increased attention has been given to the compound $La_{1-x}Ca_xMnO_3$, where the ions La^{3+} and Ca^{2+} have very similar ionic radii, e.g. 1.36 and 1.38Å respectively. The Ca doped $LaMnO_3$ manganites have a mixed valence of Mn^{3+}/Mn^{4+} with the configuration $(t_{2g})^3(e_{g1})^1$ for Mn^{3+} and $(t_{2g})^3$ for Mn^{4+}. By changing the ratio La/Ca and by varying the temperature, the transport properties of the $La_{1-x}Ca_xMnO_3$ materials can be turned from insulating to metallic state [2]. The magnetic properties can vary from paramagnetic, ferromagnetic to antiferromagnetic by changing the doping in the cationic site. In the ferromagnetic region, corresponding to a doping range of 0.3< x

< 0.7, a drop in the resistivity has been observed at the transition point from metal to semiconductor followed by the colossal magnetoresistive effect (CMR). The double exchange mechanism, which is often used to explain the CMR phenomena [3], consists of an exchange of the e_g electrons between neighboring Mn ions loading.

Traditionally, these mixed oxides have been prepared through a calcination-milling (CM) procedure, leading to low surface area, and poorly active materials. To overcome this limit, several techniques were developed, among which the so-called citrate or tartrate sol–gel (SG) method allows to obtain relatively high surface area, up to two orders of magnitude higher than those for the samples prepared by CM [4,5]. Indeed, the formation of the citrate or tartrate complex keeps the cations homogeneously dispersed, allowing obtaining the pure perovskitic phase at low calcination temperatures (ca. 500–600ºC). Thus activity of the SG samples is usually high, due to the high surface area. However, these catalysts are easily sintered, because of the very low particle size of the powder obtained at a low temperature. Thermal stability can be made sufficient for catalytic flameless combustion (CFC) application only after calcination at least at 850–900ºC, but this strongly depresses surface area [5].

It is well known [6,7] that catalytic total oxidation of hydrocarbons is supposed to occur on perovskite surface by means of a redox mechanism in which catalyst oxygen species are partly consumed by hydrocarbon and then regenerated by means of uptake from gaseous phase during a continuous cycle. Fluctuation of the Mn cation between two stable oxidation states $Mn^{3+} \leftrightarrow Mn^{4+}$ is of considerable importance for the progress of this mechanism. Moreover, different types of oxygen are involved in the oxidation process at low and high temperatures. At high temperature, the oxidation process involves lattice oxygen as active species for substituted as well as unsubstituted samples. This mechanism is connected to the presence of lattice species in the layers near the surface. Then, the evolution of these species was attributed to the reduction of the Mn site cations to lower oxidation state [8, 9].

Nevertheless, the intrinsic activity of the perovskite is difficult to clearly evidence mainly because of relatively low specific surface areas and/or presence of undesired impurities, like carbonates or oxides (e.g. Co_3O_4) [10-12]. These two parameters strongly depend on the preparation method as well as the calcination

procedure for achieving the crystallized perovskite phase. Citrate method is probably the most widespread and the most effective route to create higher surface areas. Additionally, the decomposition of the amorphous citrate precursors leads to mixed oxides or solid solutions of high homogeneity [13] contrary to methods using hydroxide precursors for instance [14].

The aim of this work is to prepare $La_{0.7}Ca_{0.3}Mn_{0.95}Fe_{0.05}O_3$ perovskites using the different preparation methods (citrate, oxalate and co-precipitated methods), evaluate their catalytic properties for hydroxylation of benzene and establish relationships with physico-chemical properties. The samples were characterized by XRD, FT-IR and SEM techniques.

Materials

Lanthanum chloride ($LaCl_3$), manganese nitrate ($Mn(NO_3)_2$), calcium nitrate ($Ca(NO_3)_2$), ferric nitrate ($Fe(NO_3)_3$), citric acid, oxalic acid, ammonium carbonate and ethylene glycol were purchased from Merk company. Benzene, hydrogen peroxide, ammonium hydroxide, 4-amino-antipyren and potassium ferricyanide ($K_3[Fe(CN)_6]$) were purchased from Sigma company.

Experimental

Preparation of perovskites by sol gel methods [15]

a) Gel–citrate complexation route (GC sample)

The perovskites particles were prepared by the citrate precursor method. Briefly, the gel precursor was prepared as follows. 0.7mol $LaCl_3.5H_2O$, 0.3mol $Ca(NO_3)_2$ 0.95mol $Mn(NO_3)_2$, 0.05 mol $Fe(NO_3)_3{\cdot}9H_2O$, and 0.2 mol $C_6H_8O_7{\cdot}H_2O$ as quilting agent were dissolved in 400 ml of deionized water. The solution was stirred for 1 h at 80ºC. Ethylene glycol (0.1mol) was added to the previous solution with continuous stirring until a viscous gel was formed. The resulting gel was evaporated till dryness. The gel pieces were ground to form fine powders. The powders were pressed and then calcined at 900 ºC for 12 h.

b) Gel–oxalate complexation route (GO sample)

Stoichiometric amount of $LaCl_3$ and Ca, Mn and Fe nitrates were dissolved in distilled water. Then a solution of oxalic acid in water was added to the metal solution with vigorous stirring. The oxalic acid/metal ions ratio (La, Ca, Mn, and Fe) was fixed at 2:0.7:0.3:0.95:0.05, respectively. The solution was stirred for 1 h at 80ºC and then ethylene glycol (0.1mol) has been added to the previous solution with

continuous stirring until a viscous gel was formed. The resulting gel was evaporated till dryness. The gel pieces were ground to form fine powders. The powders were pressed and then calcined at 900 ºC for 12 h.

Co-precipitation route (CP sample)

The $La_{0.7}Ca_{0.3}Mn_{0.95}Fe_{0.05}O_3$ perovskites were prepared by the co-precipitation method. Stoichiometric amounts of $LaCl_3$ and Ca, Mn and Fe nitrates were dissolved in water under vigorous stirring for 1 h at 70ºC. A solution of ammonium carbonate has been added dropwise to the previous solution. The precipitate was formed and has been checked for complete precipitation by adding few drops of ammonium carbonate to the mixture. Afterwards, the precipitate was filtered, dried at 120 °C for 4 h, the powders were pressed and then calcined at 900 °C for 12 h in a static oven.

Physico-chemical characterizations

Powder X-ray diffraction (XRD) data of the prepared samples were measured at room temperature by using a Philips diffractometer (type PW 3710). The patterns were run with Ni-filtered copper K_α radiation (λ = 1.5404Å) at 30 kV and 10 mA with a scanning speed of 2θ = 2.5º/min. Rietveld analysis of the diffraction data was performed using the FULLPROF program. The size of the crystallographic grain has been deduced by applying the Scherrer formula.

Scanning electron micrographs (SEM) were obtained on a Joel scanning microscope model JSM5410 operated at 15 kV. The sample was deposited on a sample holder with an adhesive carbon foil and sputtered with gold.

Catalytic tests

The reaction was carried out in a solvent-free three-phase slurry reactor system. This liquid phase reaction was conducted in a 250 ml batch glass reactor equipped with a condenser under atmospheric pressure. A hotplate-magnetic stirrer with variable speed and an oil bath were used for stirring and heating the mixture. The catalyst was dried at 383 K prior the reaction. A typical reaction mixture contained 0.1g of catalyst, 50cm^3 of benzene (99.7%) and 2cm^3 of H_2O_2 solution (30% wt/wt) was added dropwise during 30 min with stirring for about 70 min. Then, the concentration of phenol was determine at λ_{max} = 510 nm using a spectrophotometer by the 4-aminoantipyrene method [16,17] as follows; 0.5mL of 4-aminoantipyrene was added into supernatant solution. 0.5mL of $K_3[Fe(CN)_6]$ was added into the

previous mixture. After 15 min, the absorbance at λ_{max} = 510 nm was determined, then the concentration of phenol can be calculated. The phenol selectivity based on benzene (SPhen/SC_6H_6) is defined as the molar ratio of the formed phenol to converted benzene. The selectivity based on H_2O_2 is defined as the molar ratio of the formed phenol to hydrogen peroxide consumption (SPhen/SH_2O_2).

Results and discussion

Phase homogeneity

Phase homogeneity of $La_{0.7}Ca_{0.3}Mn_{0.95}Fe_{0.05}O_3$ materials was evaluated by comparison with the structural data reported in the literature [18-20]. $La_{0.7}Ca_{0.3}Mn_{0.95}Fe_{0.05}O_3$, like all $La_{1-x}Ca_xMnO_3$ systems with x<0.5, crystallizes in a rhombohedral structure (**R3̄c** space group). The rhombohedral distortion of the ideal perovskite octahedra is characterized by the splitting of the principal reflection, which appears as a double peak in the range of 2θ =32–34°.

Fig. 1 shows the XRD patterns of $La_{0.7}Ca_{0.3}Mn_{0.95}Fe_{0.05}O_3$ prepared with the three investigated synthetic methodologies. For clarity, the expansion at 2θ = 31–35° range is shown in the inset. The material prepared via gel–oxalate (GO sample) shows single-phase character with the presence of weak diffraction peak at 2θ=35.6°, due to the precipitation of a very small amount of cubic Mn_3O_4 [JC-PDF, card No75-0033]. This indicates that the GO process under the adopted conditions is not able to produce a homogeneous material and the rhombohedral phase of $La_{0.7}Ca_{0.3}Mn_{0.95}Fe_{0.05}O_3$ is formed by solid state reaction of the constituents of the combustion “ashes”. Notably, the gel–oxalate process has been widely used to prepare $LaNi_xFe_{1-x}O_3$ nanoparticles with good phase homogeneity [21]. Therefore, for the presented $La_{0.7}Ca_{0.3}Mn_{0.95}Fe_{0.05}O_3$ sample, we can not exclude that the synthetic conditions, such as oxalic/metal ions ratio, can be further optimized leading to homogeneous materials.

The material prepared through the gel–citrate (GC sample) and the co-precipitation (CP sample) routes present the desired phase even after calcination at low temperature: the fit of XRD patterns of GC and CP samples is in a good agreement with the rhombohedral structure of $La_{0.7}Ca_{0.3}Mn_{0.95}Fe_{0.05}O_3$. This result is consistent with the statistical distribution of the cations in the resin produced by GC synthesis and in the mixed hydroxides produced by CP synthesis, which is maintained in the final materials.

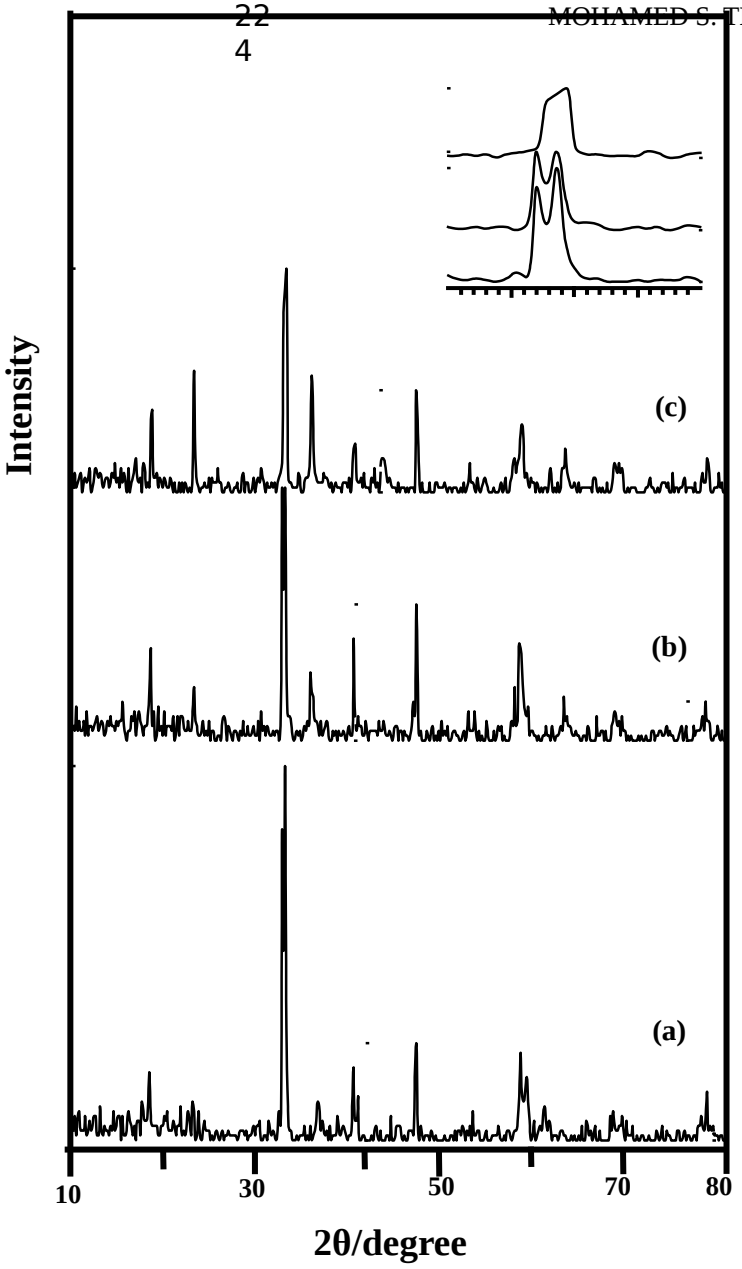

Fig. 1: X-ray diffractograms of proviskite materials prepared by different methods and calcination at 900°C, where (a) co-precipitation method, (b) Citrate method and (c) oxalate method

A careful analysis of two important diffraction peaks (located at 2θ =33º and 57º) shows the changes in the crystalline structure of this series. A close up of the signal corresponding to 2θ =33º is also shown in Fig. 2. It can be observed that the two signals studied for the perovskites prepared with GO are singlets. The first, at 33º is acute and intense, while the one at 57º is wide with a much less intensity, typical of orthorhombic structures.

The perovskite prepared with gel–citrate and co-precipitation presents different behavior, indicating that the structure changes since the signal at 33º presents a small doublet and the singlet at 57º presents a shoulder at 58º characteristic of rhombohedral systems. For the perovskites prepared with gel–citrate and co-precipitation methods, the structure is rhombohedral. The lines of the values of 2θ =33º is an acute, very intense doublet that is separated for close to 0.02º, while the second one at the 57º presents a shoulder at 58º and is wide with a low intensity. These results suggest that the perovskite prepared with GC and CP is formed with these methods.

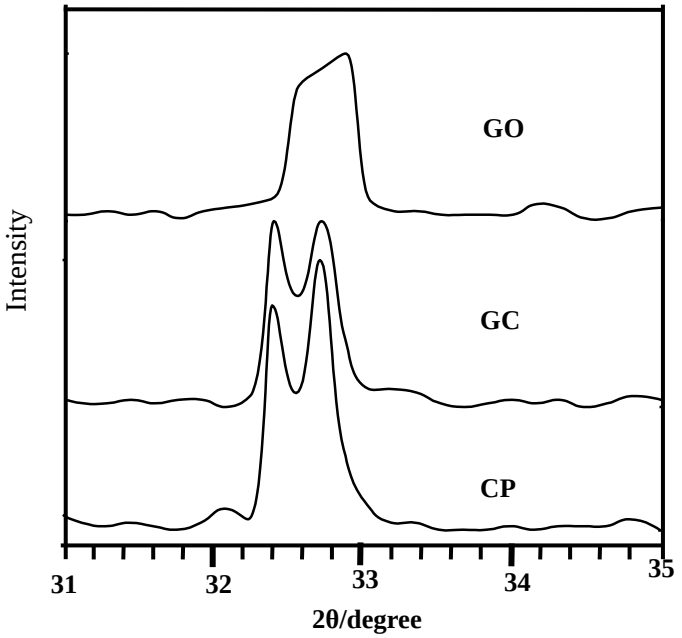

Fig.2. XRD diffractograms of $La_{0.7}Ca_{0.3}Mn_{0.95}Fe_{0.05}O_3$ samples, collected after the calcination treatment at 9000ºC.
As a reference: the positions of the reflection of the cubic (JC-PDF, card No. 750541) and orthorhombic (JC-PDF, card No. 742203) $LaFeO_3$ and cubic (JC-PDF, card No. 330710) and rhombohedral (JC-PDF, card No. 330711) $LaNiO_3$ phase are reported.

The perovskite prepared with gel–citrate and co-precipitation presents different behavior, indicating that the structure changes since the signal at 33º presents a small doublet and the singlet at 57º presents a shoulder at 58º characteristic of rhombohedral systems. For the perovskites prepared with gel–citrate and co-precipitation methods, the structure is rhombohedral. The lines of the values of 2θ =33º is an acute, very intense doublet that is separated for close to 0.02º, while the second one at the 57º presents a shoulder at 58º and is wide with a low intensity. These results suggest that the perovskite prepared with GC and CP is formed with these methods.

The Reitveld analysis of the pattern shows that the crystal structures of three samples were rhombohedral with space group $R\bar{3}C$ (Fig.3), from which, the lattice parameters, unit cell volume and particle size are calculated in (Table 1). The samples prepared by co-precipitation or citrate methods have the same lattice parameters (Table 1). These results demonstrate the replacement of Mn by Fe without any structural change and that the lattice effects have indeed been by passed. The results are consistent with Jonker's earlier conclusion [22, 23] that Mn^{3+} is replaced by Fe^{3+} of the same size in the octahedral coordination.

Scanning electron microscopy (SEM)

In order to study the microstructure of the synthesized perovskites prepared by different methods, SEM examinations were performed. Fig. 4 (a–c) shows the SEM micrographs obtained for all samples which exhibited foamy agglomerated particles with a wide distribution and presence of large voids in their structure. A strongly aggregated morphology was observed for powders prepared using the oxalate precursors (a). In case of the powders obtained starting with oxalate (b), pieces of gel were obtained while in the case of powders obtained starting with citrate method (c) a more dispersion was obtained. This result strongly supports that the citrate method plays a structure directing role enhancing the nucleation. The enhanced nucleation has thus led to the formation of smaller crystals.

FT-IR spectroscopy

Fig.5 presents the IR spectra obtained for all the perovskites in the zone between 4000 and 500 cm^{-1}. The wide band at 3600 cm^{-1} is associated to the lengthening of water's O-H bond due to exposure to air and environmental humidity for the studied perovskites. The broad band in the spectrum obtained for sample prepared by OG is observed at 2988 cm^{-1} and a small band at 2420 cm^{-1}, which corresponds to a vibration mode v_3 of the CO_3^{2-} groups that are essentially asymmetrical with symmetrical lengthenings of the O-C-O bond [24] due to the presence of segregated phases in the form of carbonates.

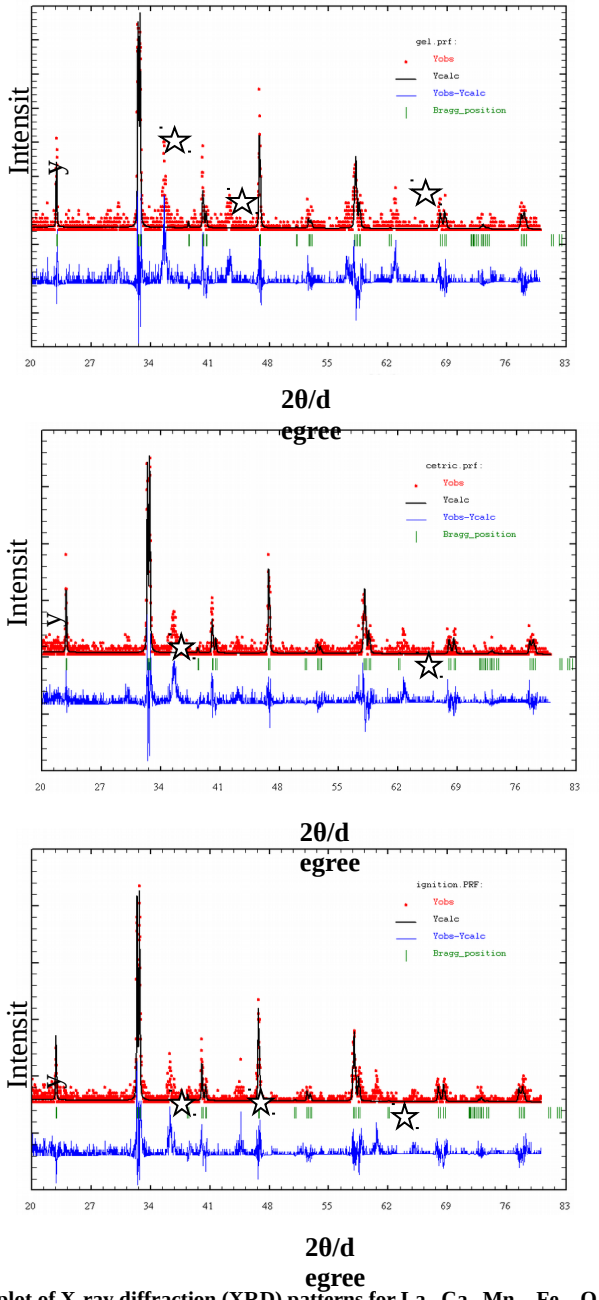

Fig. 3. Rietveld plot of X-ray diffraction (XRD) patterns for $La_{0.7}Ca_{0.3}Mn_{0.95}Fe_{0.05}O_3$ samples. Reddots indicate the experimental data and the blacklines overlapping them indicate calculated profiles. The lowest curve shows the difference between experimental and calculated patterns. The vertical bars in green are the expected Bragg's positions. The peak with star is attributed to the Mn_3O_4

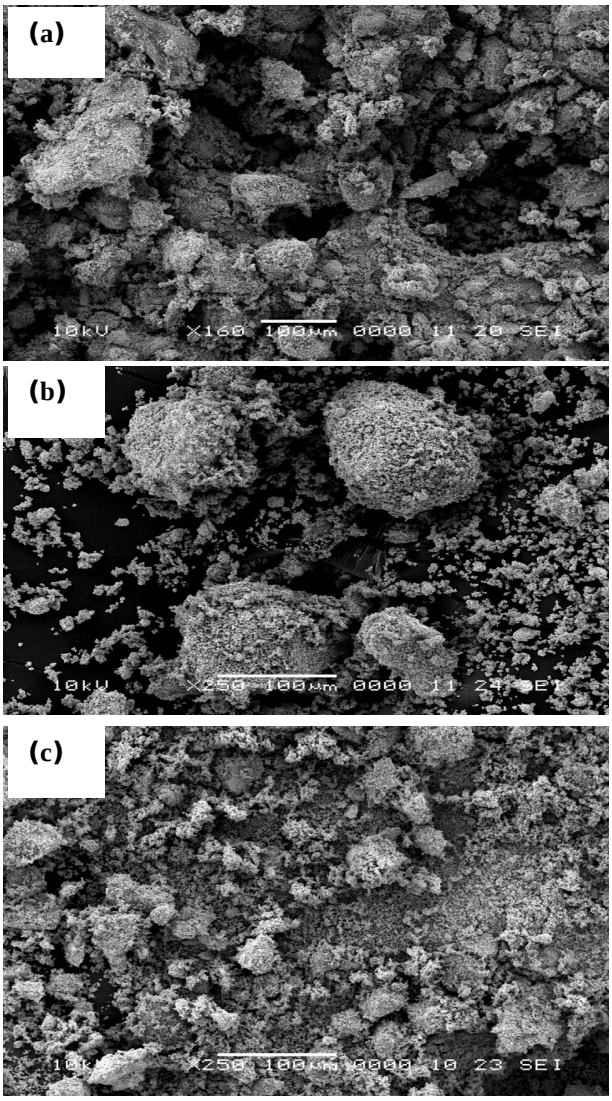

Fig. 4. SEM micrographs of different proviskite samples prepared by (a) co-precipitation; (b) oxalate method and (c) citrate method

Table 1: Structure parameters for $La_{0.7}Ca_{0.3}Mn_{0.95}Fe_{0.05}O_3$ samples

Samples	Cell parameters			V (Å)^3
	a	b	c	
co-precipitation	5.5160	5.5160	13.3557	351.9168
Citrate methods	5.5100	5.5100	13.3497	350.9939
oxalate methods	5.4990	5.4990	13.3387	349.3058

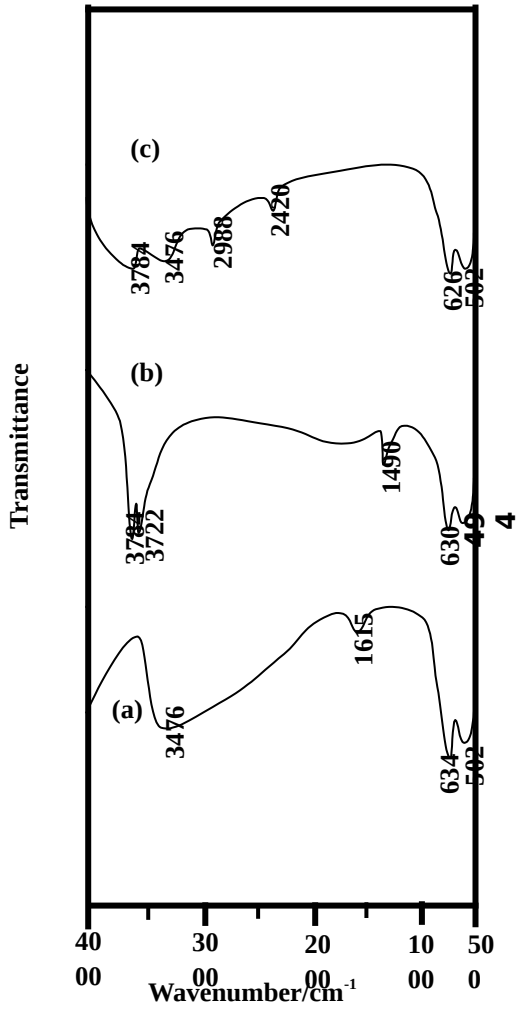

Fig. 5: FT-IR spectra of proviskite prepared by (a) co-precipitation (CP) (b) oxalate method (GO) and (c) citrate method (GC).

The most important band of the perovskites structure (Fig.3) v_1 is observed at 630 cm^{-1}, which is the characteristic band of oxides with perovskite-type structure. The absorption peaks observed around ν_3 at ~630cm^{-1} and ν_4 at ~500cm^{-1} should belong to stretching, ν_3 and bending, ν_4 of the internal modes of MnO_6 octahedral [25-27]. The stretching mode is related to the change of Mn–O–Mn bond length and the bending mode which involves the change of Mn–O–Mn bond angle. The appearance of the stretching and bending modes at transmission spectra indicates that the perovskite structure of LSMO has been formed at temperature of 800 ºC, which is in agreement with the result of XRD shown in Fig. 1.

Catalytic activity

Oxidation reactions on oxides are often described by means of the Mars and van Krevelen model [28,29] involving a two step redox reaction mechanism; the first one is the reaction between the oxidisable reactant (hydrocarbon) and the active oxygen on the surface and the second one is the re-oxidation of the reduced surface site by gas phase oxygen. It is well known [6,7] that catalytic total oxidation of hydrocarbons is supposed to occur on perovskite surface by means of a redox mechanism in which catalyst oxygen species are partly consumed by hydrocarbon and then regenerated by means of uptake from gaseous phase during a continuous cycle. Fluctuation of the Mn cation between two stable oxidation states $Mn^{3+} \leftrightarrow Mn^{4+}$ is of considerable importance for the progress of this mechanism. Moreover, different types of oxygen are involved in the oxidation process at low and high temperatures. At high temperature, the oxidation process involves lattice oxygen as active species for substituted as well as unsubstituted samples. This mechanism is connected to the presence of lattice species in the layers near to surface. Then, the evolution of these species was attributed to the reduction of the Mn site cations to lower oxidation state [30, 9]. At low temperature, weakly adsorbed or surface oxygen species are involved.

Figure 6 shows the behavior of the phenol yield with increasing reaction time. The yield of phenol reaches the maximum values of 15.5, 20.7 and 25.4% over the three samples of CP, OG and CG, respectively, at a reaction time of 60 min. The maximum conversion on CG methods may be related to the high homogeneity and the high surface area of this sample.

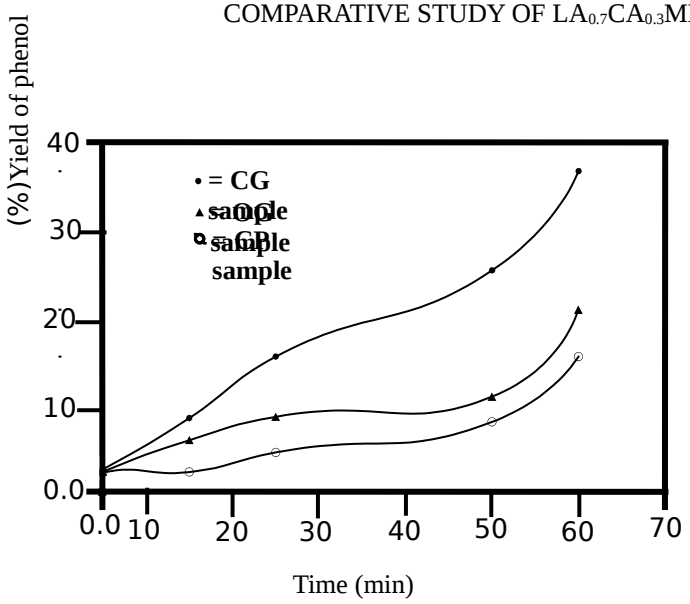

Fig. 6: Yield of phenol produced on different samples prepared by different methods. Reaction conditions: atmospheric pressure, temperature 80 °C, catalyst 0.1 g, ratio of H_2O_2 to benzene equal 0.0388 mole, 20 ml additional water, reaction time 60 min.

The effect of the amount of H_2O_2 on the yield of phenol over the citrate sample is shown in Fig. 7. H_2O_2 acts as the oxidant in the conversion of benzene to phenol. Thus, it is natural that no phenol is obtained without H_2O_2. The variation of phenol yield with the amount of H_2O_2 used gives the same tendency over the three catalysts used; i.e., the yield of phenol increases along with the increase of the amount of H_2O_2 and reaches a maximum at 38.8 mmol (1.85 mol l^{-1}) H_2O_2; this corresponds to a molar ratio of H_2O_2 to benzene of about 1.7. A slight decrease in the yield of phenol was observed with further increase of the amount of H_2O_2 over this molar ratio. This may result from the further oxidation of the formed phenol.

The stoichiometric ratio of H_2O_2 to benzene for the hydroxylation reaction is 1:1, while the results show that the H_2O_2 needed for the favorable phenol yield is about two times its stoichiometry. In fact, in the present reaction system, the benzene catalyzed oxidation is accompanied by the self-decomposition of hydrogen peroxide. Therefore, the excess of H_2O_2 may be consumed in the deep oxidation or in its self-decomposition. The selectivity of H_2O_2 is quite low; thus, the enhancement of the effective use of H_2O_2 in the present reaction system offers a further challenge.

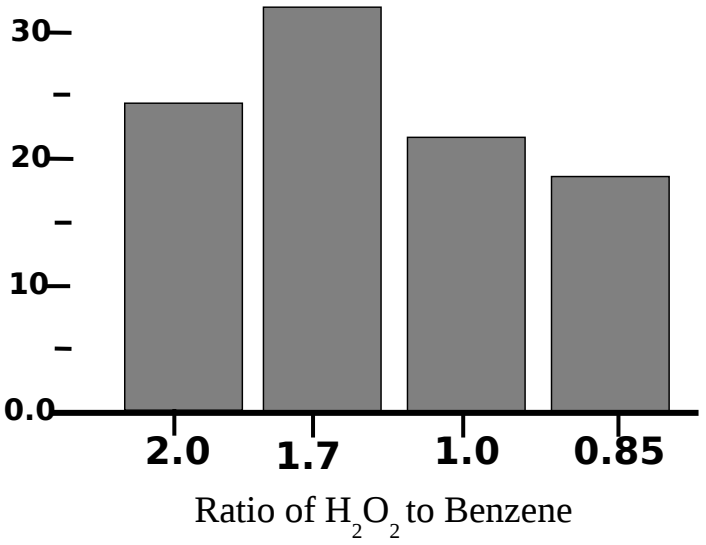

Fig.7: H_2O_2 conversion to organic compounds and product selectivity as a function of molar ratio of benzene/H_2O_2 in the benzene hydroxylation catalyzed by citrate–gel method. Reaction conditions: atmospheric pressure, temperature 80 ºC, catalyst 0.1 g, 0.0388 mole of H_2O_2 and x mole of benzene (x =0.0194, 0.0228, 0.038and 0.045 mole), 20 ml additional water, reaction time 60 min

Conclusions

Single-phase $La_{0.7}Ca_{0.3}Mn_{0.95}Fe_{0.05}O_3$ perovskites nanoparticles were prepared by the sol–gel process and its structural and catalytic properties were investigated. From the present results it can be concluded that the sol–gel method using citric acid as a chelating agent proved to be useful for the preparation $La_{0.7}Ca_{0.3}Mn_{0.95}Fe_{0.05}O_3$ perovskites than the other two methods. In addition, the activities of the samples prepared through co-precipitation or oxalate methods were lower than that obtained with citrate method; this indicates that catalytic activity correlates not only with the bulk structure of the perovskite phase, and consequently oxygen mobility, but also with the content of manganese and its surface concentration.

References

1. K.H. Ahn, X.W. Wu, K. Liu and C.L. Chien. Phys. Rev. B., 54 (1996) 15299.

2. M. Ziese, H.C. Semmelhack, K.H. Han, S.P. Sena, and H.J. Blythe. J Appl. Phys., 91(2002) 9930.

3. C. Zener. Phys. Rev., 82 (1951) 403.

4. H.M. Zhang, Y. Teraoka and N. Yamazoe, Chem. Lett., (1987) 665.

5. H. Arai, T. Yamada, K. Eguchi and T. Seiyama, Appl. Catal., 26 (1986) 265.

6. T. Seiyama, in: L.G. Tejuka, J.I.G. Fierro (Eds.), Properties and Applications of Perovskite-type Oxides, Marcel-Dekker, NY, (1993) 215.

7. L.G. Tejuka, J.L. Fierro and J.M.D. Tascon, Adv. Catal., 36 (1989) 237.

8. R.J.H. Voorhoeve, Advanced Materials in Catalysis, Academic Press, NY, (1977) 129.

9. T. Seiyama, N. Yamazoe and E. Eguchi, Ind. Eng. Chem. Prod. Res. Dev., 24 (1985) 19

10. J.-J. Liang and H.-S. Weng, Ind. Eng. Chem. Res., 32 (1993) 2563–2572

11. G. Busca, M. Daturi, E. Finocchio, V. Lorenzelli, G. Ramis and R.J. Willey, Catal. Today, 33 (1997) 239–249.

12. S. Royer, F. Berube and S. Kaliaguine, Appl. Catal. A: Gen., 282 (2005) 273–284.

13. M. Alifanti, J. Kirchnerova and B. Delmon, Appl. Catal. A: Gen., 245 (2003) 232–243.

14. K.R. Barnard, K. Foger, T.W. Turney and R.D. Williams, J. Catal., 125 (1990) 265-275.

15. M. Bevilacqua, T. Montini, C. Tavagnacco, G. Vicario, P. Fornasiero and M. Graziani, Solid State Ionics, 177 (2006) 2957–2965

16. A.E. Greenberg, L.S Clesceri, and A.D. Eaton (Eds.), Standard Methods for the Examination of Water and Wastewater, 17th ed., American Public Health Association (APHA), Washington, DC, (1989).

17. Ali Tor, Yunus Cengeloglu, Mehmet Emin Aydin and Mustafa Ersoz**,** J. Colloid and Interface Science, 300 (2006) 498–503

18. S. Rousseau, S. Loridant, P. Delichere, A. Boreave, J.P. Deloume and P. Vernoux, Applied Catalysis B: Environmental, 88 (2009) 438–447

19. Darshan C. Kundaliya, Reeta Vija, R.G. Kulkarnia, A.A. Tulapurkar, R.Pinto, S.K. Malik and W.B. Yelon, Journal of Magnetism and Magnetic Materials, 264 (2003) 62–69.

20. E. K. Abdel-Khalek, W M EL-Meligy, E.A. Mohamed, T. Z. Amer and H. A. Sallam, J. Phys.: Condens. Matter, 20 (2008).

21. E. Bontempi, C. Garzella, S. Valetti and L.E. Depero, J. the European Ceramic Society, 23 (2003) 2135–2142.

22. G.H. Jonker, Physica (Amsterdam), 20 (1954) 1118.

23. A.G.Mostafa, E.K.Abdel-Khalek, W.M.Daoush and S.F.Moustfa, J. Magnetism and Magnetic Materials, 320 (2008) 3356–3360.

24. G. Pecchi, C. Campos, O.Pena and Luis E. Cadus, J. Mol. Catal. A, 282 (2008) 158–166.

25. Wein-Duo Yang, Yen-Hwei Chang and Shu-Hui Huang, J. Eur. Ceram. Soc., 25 (2005) 3611.

26. B.M. Nagabhushana, R.P. Sreekanth Chakradhar, K.P. Ramesh, V. Prasad, C. Shivakumara and G.T. Chandrappa, Physica B, 403 (2008) 3360.

27. A.Rostamnejadi, H. Salamati, ParvizKameli and H. Ahmadvand, J.Magnet. & Magnet. Mater., 321 (2009) 3126–3131.

28. P. Mars and D. Van Krevelen, Chem. Eng. Sci. Suppl., 3 (1954) 41.

29. R. Hammami, S. Ben Aıssa and H. Batis Appl. Catal. A, 353 (2009) 145–153.

30. R.J.H. Voorhoeve, Advanced Materials in Catalysis, Academic Press, NY, (1977) 129.